Proximity Effects in Electron Lithography: Magnitude and Correction Techniques

Proximity effects due to electron scattering in the resist and substrate seem to set a fundamental limit to the areal density that can be achieved in electron lithography. This work briefly reviews the form and the magnitude of the proximity function and its extent as evidenced by deviations in designed linewidths. It also discusses methods to decrease the proximity effect as well as the algorithms used for correction of such effects.

Introduction

The proximity effect [1-8] in electron lithography refers to undesired exposure of a resist in regions adjacent to those actually addressed by the electron beam (e-beam). The manifestation of this undesired exposure is that some shapes [9] develop less completely than others. If development is allowed to proceed until all shapes are completely developed, some shapes may be larger than designed, while gaps between shapes may be smaller than designed or even nonexistent.

Figure 1 (a) Optical micrograph of an uncorrected pattern showing underdevelopment due to intrashape proximity effects at point A and at points C and D. Overdevelopment due to intershape proximity effect is seen at point E. (b) Optical micrograph of a SPECTRE-corrected pattern shown in (a). Dissection of a complex pattern into (c) 13 rectangles and (d) 21 rectangles.

Figure 1 [especially Fig. 1(a)] illustrates this effect. The small shape A remains underdeveloped, while regions within the large shape B are completely developed. Long shapes adjacent to large shapes are especially susceptible to problems since parts of such shapes not in proximity to other shapes, e.g., C and D, are underdeveloped, while parts adjacent to large shapes are overdeveloped. This leads to decreases in the gaps between shapes E. Further development of such a pattern can result in the closing of such gaps.

The fundamental aim of any proximity effect correction technique is to provide all shapes in the pattern with approximately the same level of development (i.e., the same type of wall profile). The type of wall profile is determined almost exclusively by the exposure and/or development conditions. For example, if certain exposure conditions were to yield sloping walls in a nominal 5- μ m pattern, a proximity correction technique would attempt to reproduce such wall profiles in all shapes (especially in smaller ones) in the pattern.

Proximity function and the extent of its effect

Phenomena

The developed image in the resist is formed through the cumulative action of several physical phenomena. They can be delineated as 1) scattering of incident and secondary electrons in the resist and substrate, 2) energy deposition in the resist and concomitant restructuring of the resist molecules, and 3) action of the developer on the

Copyright 1980 by International Business Machines Corporation. Copying is permitted without payment of royalty provided that (1) each reproduction is done without alteration and (2) the *Journal* reference and IBM copyright notice are included on the first page. The title and abstract may be used without further permission in computer-based and other information-service systems. Permission to *republish* other excerpts should be obtained from the Editor.

molecules in the resist. Some of these processes have been modeled in detail. The interested reader is referred to Refs. [4-6] for discussions of electron scattering and energy deposition in electron resists on substrates. Models of developer action on irradiated resists are discussed in Refs. [10-11]. In this paper we restrict our interest to the *net* influence in the resist of all these phenomena. Thus, we can disregard the details of each of these processes if a formulation describing the cumulative process can be defined.

• Proximity function

The proximity function is defined as a point-spread function relating the "influence" in the resist at a point at a distance r from the point of incidence of the beam. This influence is the cumulative action of all the phenomena discussed previously and has also been referred to as resultant exposure [8], effective exposure [12], specific fragmentation (see Ref. [13], specifically [13a]), etc. Based on the calculations of electron scattering and energy deposition studies [4-6], it has been postulated [7] that the proximity function f(r) can be approximated by the sum of two Gaussian functions related to the influences of the forward (characteristic width β_p) and backward (characteristic width β_b) scattered electrons [see Fig. 2]. Thus, the proximity function can be written [8, 13a] as

$$f(r) = k \left[\exp\left(-r^2/\beta_{\rm f}^2\right) + \eta_{\rm F} \beta_{\rm f}^2/\beta_{\rm b}^2 \exp\left(-r^2/\beta_{\rm b}^2\right) \right],\tag{1}$$

where k is a constant and η_E is the ratio of integrated contributions of backscattered to forward-scattered electrons. The detailed derivation of this equation can be found in Ref. [14]. One fundamental assumption made in deriving Eq. (1) is that the distribution of energy deposition is directly related to the distribution defined by the proximity function; see Ref. [15] for further discussion of this assumption. A Monte Carlo simulation of electron energy deposition has shown [14] that a Gaussian function serves as a good approximation for the backscattered electron distribution from a silicon substrate. For high atomic weight substrates like copper and certainly gold, the backscattered distribution needs to be described by two Gaussians [14]. While the forward-scattered distribution at the surface of the film cannot [16] be described by a Gaussian, one finds it to be a fair approximation at the resist-substrate interface. Recent calculations [17] indicate that two Gaussians yield an even better approximation to the forward-scattered distribution, especially when the incident electron beam diameter is small. For mathematical simplicity one generally considers only a two-dimensional proximity function (i.e., independent of z, the distance into the resist from the surface). Thus, one assumes that f(r) is either appropriately averaged over all z in the resist, or is considered for a particular value of z(e.g., at the resist-substrate interface).

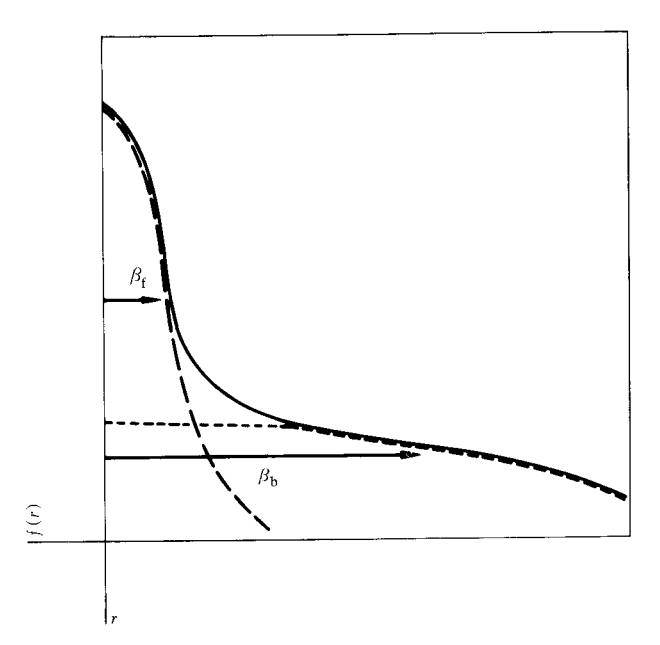


Figure 2 Schematic of the proximity function. The forward-scattered distribution (———) has characteristic width $\beta_{\rm f}$, while the backscattered distribution (——) has characteristic width $\beta_{\rm b}$.

Table 1 Proximity function parameters for silicon substrates.

Ref.	Resist thickness (µm)	Electron energy (keV) [♦]	$eta_{_{\mathrm{f}}}^{st}$ $(\mu\mathrm{m})$	$\begin{pmatrix} eta_{ m b} \\ (\mu{ m m}) \end{pmatrix}$	$\eta_{_{ m E}}$
 [5b]	1.0	20		2.5 [†]	_
[8]	0.6	25	0.1	1.0	0.6
[13]	0.5	25	0.06^{\ddagger}	2.6	0.51
[17]	0.6	25	0.25	2.35	0.86
[18]	1.2	20		_	0.91
[19]	0.6^{\S}	20		_	1.0
[20]	0.5	20	0.3	1.6	0.33*

^{*}Determined from c_t and $c_{\rm b}$ values

• Parameters for the proximity function

The three parameters that characterize the proximity function are $\beta_{\rm F}$, $\beta_{\rm b}$, and $\eta_{\rm E}$. These can in principle be obtained either from theory or experiment [12, 13c, 14, 18–20]; however, there is considerable discrepancy and controversy over these values. Table 1 shows a compendium of the parameters for the case of 20–25-keV electrons incident on resist films on Si. The various values of $\beta_{\rm f}$ are admittedly difficult to compare, since the reported values depend on the incident e-beam diameter β^* . Since $\beta_{\rm b}$ is very weakly affected by β^* , it can be used to make more

[†]Deduced from graphic data.

[‡]Except for the data from Ref. [14] for a point source. β_f implicitly involves a convolution of the incident beam distribution with the forward-scattering distribution. §Copolymer, COP.

 $^{^{\}circ}$ 1 keV = 1.602 × 10⁻¹⁶ J. Throughout text energy values are given in keV.

direct comparisons between the values of various workers [8, 13c, 20]. The parameter $\eta_{\rm E}$ is also subject to controversy [8, 12, 14, 18-19]. The reason for these differences in $\beta_{\rm b}$ and $\eta_{\rm E}$, whether due to differences in exposure or developer conditions, is at present unclear. We propose the *adoption* of a set of values that may be operationally useful (i.e., their use gives "adequate" results) for the lithographic conditions noted in Table 1. These are: $\beta_{\rm f} \approx 0.1~\mu{\rm m}$, $\beta_{\rm b} \approx 2.5~\mu{\rm m}$, and $\eta_{\rm E} \approx 0.9$.

The trends in the behavior of these parameters for different electron lithographic conditions (e.g., beam energy, resist thickness, substrate material, etc.) can be estimated from theoretical calculations [14]. The value of β_c is expected to increase with increasing resist thickness or with increasing depth into the resist, to decrease with increasing beam energy, and to be essentially independent of the substrate material. On the other hand, since $\beta_{\rm h}$ seems [14] to be monotonically related to the range of electrons in the substrate, it decreases dramatically with increasing atomic weight of the substrate. (When the backscattered distribution becomes bimodal, two parameters are required.) It also increases with increasing beam energy and is weakly influenced by the resist thickness or material. The value of $\eta_{\rm E}$ increases with increasing atomic weight [14, 18, 19] of the substrate and is only weakly dependent on resist thickness [14]. The relatively weak dependence of both β_b and η_E on the resist thickness further substantiates the previously discussed assumption that the proximity function is independent of z.

• Magnitude of the proximity effect

The magnitude of the proximity effect can be assessed by calculating the influence ε in the resist at a point r_i due to the writing of a complex pattern (consisting of m shapes, each with area A_i):

$$\varepsilon(\mathbf{r}_i) = \sum_{J=1}^m \int_{A_J} f(r_{ij}) dA_J; \qquad r_{ij} = |\mathbf{r}_i - \mathbf{r}_j|. \tag{2}$$

These values of ε at particular points in the pattern can be used to determine deviations from designed pattern dimensions. Thus, an estimate of the magnitude of the proximity effect can be obtained for a given proximity function. The deviations from the designed pattern dimensions have been calculated as shown in Ref. [21]. On the basis of these data, the following generalizations can be made: 1) The dimensional deviations seem to be only weakly dependent on the exact magnitude of β_b as long as it lies in the range ≈ 1.0 –2.5 μ m. However, when β_b is $\approx 5 \mu$ m, the dimensional deviation seems to decrease significantly. 2) The role of η_E is difficult to assess: its influence seems to be related to the magnitude of β_b . For example, large values of both η_E and β_b lead to significant dimensional deviations for designed linewidths ℓ_d of

1-2 μ m. For smaller β_b (\lesssim 1.0 μ m), however, large dimensional deviations are not obtained even for $\eta_E \approx 1.0$. 3) The parameter β_f strongly determines dimensional deviations and edge definition of patterns with $\ell_d \lesssim 1 \ \mu$ m. Since β_f is determined by incident e-beam diameter and the forward spreading of the beam in the resist (via resist thickness and composition), these latter quantities are critical for submicron lithography.

One can conclude that even for a finely focused beam and a sufficiently thin resist film (yielding a cumulative $\beta_f \approx 0.1~\mu\text{m}$), the proximity effect will be significant enough to lead to dimensional deviations for geometries as large as $\approx 1~\mu\text{m}$. If the beam is larger and/or the film thicker, the proximity effect may be evident even at dimensions as large as $\approx 2~\mu\text{m}$.

• Methods for decreasing the proximity effect

Basically, two types of schemes can be used to decrease the magnitude of the proximity effect. The first consists of changing the incident electron beam energy; the second, of changing the substrate and/or the resist composition and thickness. Both methods rely on altering the magnitude and distribution of energetic electrons in the resist to obtain a decrease in the proximity effect.

Incident e-beam energy Theoretically it is predicted that a significant decrease in the proximity effect may be possible with incident electron energies \gtrsim 40 keV [14, 21]. Qualitatively, such behavior can be understood as follows. An increase in incident electron energy leads [14] to an increase in the extent of the backscattered electron distribution β_b ; however, the contribution of such a distribution relative to that due to forward-scattered electrons decreases (η decreases). Thus, the proximity effect may decrease if backscattered electrons are dispersed over a large enough area for their influence at any given point to be relatively insignificant.

A decrease in the proximity effect can also be achieved by using incident electron energies of ≈ 10 keV. This has been shown [22] to be especially true in thin resist films ($\leq 0.3~\mu m$) and for pattern dimensions $\gtrsim 1~\mu m$. Qualitatively, such a behavior can be understood as follows: β_b decreases with decreasing incident electron energy. If β_b < 1 μm (the case [14] for electron energy ≈ 10 keV), little proximity effect is expected for 1- μm lithography. However, proximity effects for submicron lithography are expected to be even more severe in such a case.

Substrates Use of appropriate substrates may also lead to a decrease in the proximity effect. Investigations with substrates involving [12, 23] thin layers of high atomic number Z material sandwiched between a resist film and a

low-Z substrate have shown a potential for decreasing proximity effects. Results [23] obtained using Monte Carlo calculations for thin gold films between 1-µm PMMA and a silicon substrate (Fig. 3) show a minimum $\eta_{\rm E}$ (and thus minimum proximity effects) as the gold film thickness is increased from zero to infinity. This behavior has been at least qualitatively substantiated experimentally [12, 18–19]. A value of $\eta_E \approx 0.44$ was measured [12] for a 1- μ m PMMA film on a 350-nm Au film on garnet; while $\eta_{\rm E} \approx 0.9$ and $\eta_{\rm E} \approx 1.5$ -2.0 were measured for silicon [12] and gold [18, 19] substrates, respectively. A plausible explanation of this effect is that the presence of the high-Z (e.g., gold) film leads to a slowing down of electrons entering the substrate and a decrease in the number of electrons re-entering the resist. Thus, a film with appropriate thickness may act like a "filter" to backscattered electrons (inset in Fig. 3). Finally, investigations [21] of dimensional deviations for simple patterns indicate that for high-Z substrates the proximity effect is less than for low-Z substrates for pattern dimensions $\gtrsim 1 \mu m$. For smaller dimensions, the reverse is true.

Correction of proximity effects

• Prognosis for correction

In principle, the problem of incorrect development and subsequent linewidth variation can never be completely corrected because there is *no* means of directly controlling exposure of the resist due to scattered electrons in regions *not* addressed by the electron beam. While complete correction in all regions of the pattern may be possible, for practical electron lithographic systems it may also be unnecessary.

A viable proximity effect correction technique for a practical electron lithographic system must provide adequate compensation for proximity effects for all shapes in the pattern. Two phrases need elaboration: First, "adequate compensation" implies that only that level of proximity compensation is demanded which is physically and practically meaningful in comparison with the resolution of the lithographic system. Second, "all" shapes in a complex pattern need to be corrected, i.e., those that lie within an array as well as those that lie at the periphery of an array or are "isolated." In addition to this requirement, the following are highly desirable features of a viable proximity correction technique. First, it should be implementable for large, practical electron lithographic patterns, with only reasonable requirements on computation time and storage. Second, it should require minimal human intervention or interpretation of pattern. Computationally, the corrections should be mathematically unique and have no ambiguity based on the method of computation. Two such techniques are now discussed;

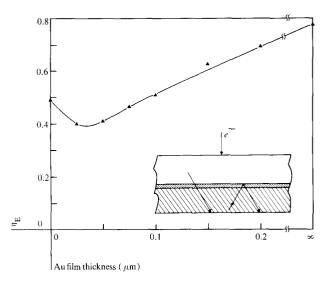


Figure 3 Monte Carlo calculated values of $\eta_{\rm E}$ as a function of the thickness of the gold film sandwiched between 1 μ m of PMMA and a silicon substrate; $E_0=25~{\rm keV}$. The inset shows "filtering" action on the backward-scattered electrons due to the gold film.

these are based on adjustments to either the pattern dimensions or the electron exposure.

• Adjustment of pattern dimensions

A technique involving changing the pattern dimensions is probably the simplest to implement on an electron lithographic machine; however, explicit determination of such changes is far from trivial. This technique is easy to utilize because only the pattern data directed to the machine are affected by proximity corrections; the operation of the machine is not affected. Thus, this technique is especially useful for machines that cannot change electron exposure from shape to shape within a pattern, e.g., an electron projection lithography machine.

Several methods have been reported for computing changes in pattern dimensions [13a, 24, 25]; all rely on the establishment of criteria for the magnitude of the proximity effect. One such criterion [24, 25] can be the value of ε [Eq. (2)] at selected "sample" points [Fig. 4] in each shape of the pattern. Another criterion [13a] can be the average value of ε over the entire shape:

$$\tilde{\varepsilon}_{I} = \int_{A_{I}} \varepsilon(\mathbf{r}_{i}) dA_{I} / A_{I}$$

$$= \sum_{J=1}^{m} \frac{1}{A_{I}} \int_{A_{I}} \int_{A_{J}} f(r_{ij}) dA_{J} dA_{I}.$$
(3)

Consider next the methods of computation and some results that are obtained when each criterion is imposed.

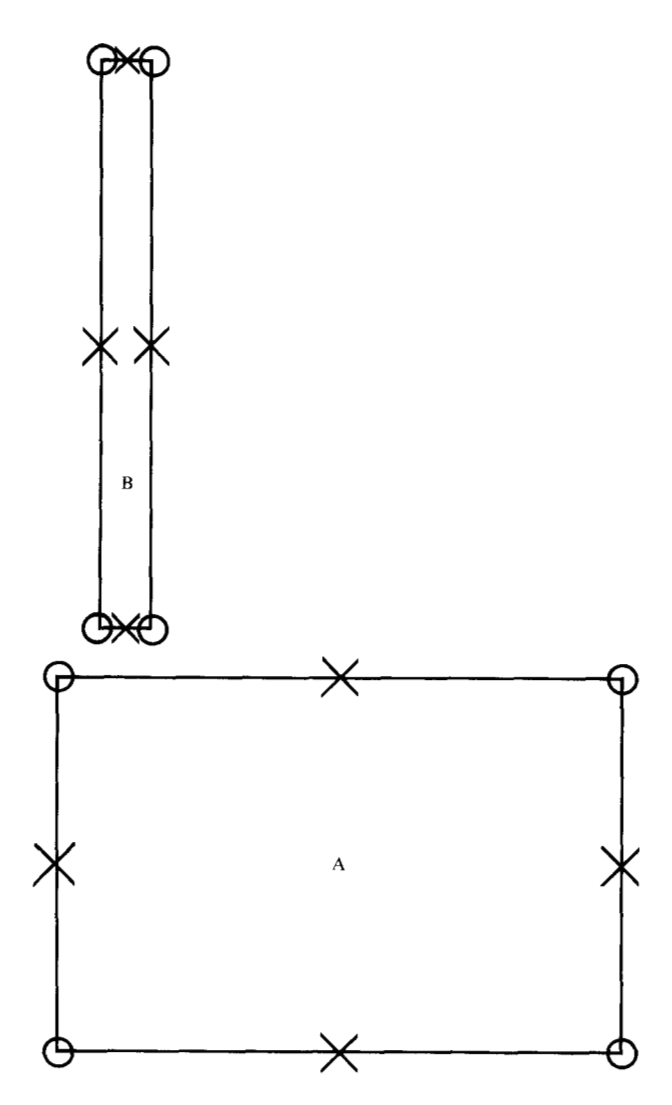


Figure 4 Schematic showing two definitions (× and O) of four "sample" points per shape in each of the two shapes of a pattern.

If the calculated values of ε at the sample points are imposed to be equal, a set of equations can be obtained whose solution yields approximations to the dimensional changes in patterns. For m shapes in a pattern, each with designed dimensions $\{x_I^d\}$ and areas A_I^d , the corrected (exposed) dimensions are $\{x_I^c\}$, each with area A_I^c . Requiring that ε at each of the n sample points in m shapes be equal to some value ε_0 , one obtains a system of s equations:

$$\varepsilon_0 \equiv \varepsilon_K(\mathbf{r}_j) = \sum_{I=1}^m \int_{A_I^e} f(r_{ij}) dA_I, \qquad K = 1, 2, \dots, s. \quad (4)$$

Here, $s = m \times n$ and is the total number of sample points where ε is considered. In principle, solutions to such equations for $\{x_I^e\}$ can be obtained in the least-squares sense since s > m. In practice [24], only a small number

of shapes ($\leq 10^2$) have been simultaneously corrected by such a technique. The solution unfortunately is not always unique; *i.e.*, a range of values of the corrected dimension $\{x_I^d\}$ yields equally good least-squares solutions to Eq. (4). In addition, the least-squares minimization and optimization requires human interpretation and interactive computing. Some may consider such requirements to be undesirable if the technique is to be used for a "black box" lithographic tool for proximity corrections.

For simple patterns such as isolated shapes and shapes adjacent to large areas, Eq. (4) can be solved exactly. In the case of isolated lines, imposing ε to be equal at the edge of a line (independent of linewidth) yields [25] exact solutions to Eq. (4), as shown in Fig. 5. Also shown (as error bars) are empirically determined values of linewidth changes that have been used [26] operationally in electron lithography. The good agreement adds credibility to the assumption of imposing equal values of ε at the edges. Application of Eq. (4) to geometries with more than one variable dimension requires [25] iterative solution of nonlinear coupled equations. For more complex geometries, ε . ε . ε , a line adjacent to a large area, graphic solutions are possible, as described in Ref. [25].

The definition of the "sample" points where ε is calculated is subject to ambiguity and is thus a source of error. This can be qualitatively seen through Fig. 4, where the two sets of placements of the four points per shape can lead to significantly different values for the intershape proximity effect that is received by shape B due to shape A. This problem can be ameliorated by consideration of the average value of ε , as defined in Eq. (3), throughout the shape, rather than values of ε at specific points. If for m shapes in a pattern, each with designed dimensions $\{x_I^d\}$ and area A_I^d , one requires the corrected (exposed) dimensions $\{x_I^c\}$ and area A_I^c , one has to impose $\tilde{\varepsilon}_I$ to be equal to, say $\tilde{\varepsilon}_0$, for all I and solve a system of m equations:

$$\bar{\varepsilon}_{0} = \sum_{J=1}^{m} \int_{A_{K}^{d}} \int_{A_{J}^{e}} f(r_{ij}) dA_{J} dA_{J} / A_{K}^{d},$$

$$K = 1, 2, \dots, m.$$
 (5)

Since such a system of equations has more unknowns $\{x_I^e\}$ than constraints m, it is found to be underdetermined. The solutions of such a system are at best arbitrary and in general, infinite. For example, in the case of two interacting rectangles, the number of unknowns can be as many as eight corresponding to the eight sides of the two rectangles, while only two equations are obtained.

If the number of dimensions in a shape that can be adjusted is reduced to only one per shape, the underdetermined system of equations in (5) becomes a fully de-

termined system of equations. This can be accomplished by a subjective human interpretation of a pattern. Alternatively, one can arbitrarily define one variable per shape. For example, if one defined k_J to be a number such that k_J^2 could be a measure of the "magnification" of a designed shape over an exposed shape, then one can write for rectangular shapes: $k_J \Delta x_J^e = \Delta x_J^d$ and $k_J \Delta y_J^e = \Delta y_J^d$. Thus, Eq. (5) becomes solvable, though not trivially. This is because of the variables k_J being embedded in the limits of the four-dimensional convolutional integral in Eq. (5).

The above discussions lead to the conclusion that while exact solutions for some simple geometries are possible, solutions for arbitrary patterns are extremely difficult to obtain even after significant approximations. In practice, empirical corrections to the designed dimensions of patterns have been deduced [26] after experimental observations of variations in pattern dimensions. While good 1- μ m pattern fidelity has been reported, such an empirical table "look-up" technique is beset with difficulties. For example [26], small variations in focusing, exposure, or development conditions can lead to large variations in pattern dimensions. Such problems can be partially minimized by defining more than one table, each optimized for a specific type or size of pattern. However, for an arbitrary pattern, ambiguity in interpretation can occur.

• Adjustment of electron exposure

Appropriate adjustment of incident electron exposure can compensate for proximity effects. Such compensation, however, relies on the benevolence of the e-beam machine. In particular, the pattern generator determines whether each shape in the pattern can be written with, if necessary, different levels of incident electron exposure, or whether sections (e.g., periphery, corners, etc.) within shapes can be written with yet other levels of exposure. Thus, with consideration of the freedom granted by the e-beam machine, a criterion based on the value of ε has to be established. As with techniques involving adjustment of pattern dimensions, we develop techniques that consider values of ε at discrete "sample" points in a shape as well as average values of ε over the area of a shape.

Calculation of ε at predefined "sample" points (Fig. 4) can lead to approximate values for exposures necessary for the compensation of the proximity effect. If for m shapes in a pattern, one defines n sample points per shape, then one obtains $s = n \times m$ equations:

$$\varepsilon(\mathbf{r}_i) = \sum_{I=1}^m n_I \int_{A_I} f(r_{ij}) dA_J, \qquad I = 1, 2, \dots, s,$$
 (6)

where n_i is the incident electron exposure (in electrons or coulombs per unit area) for shape m. If each of the $\varepsilon(\mathbf{r}_i)$

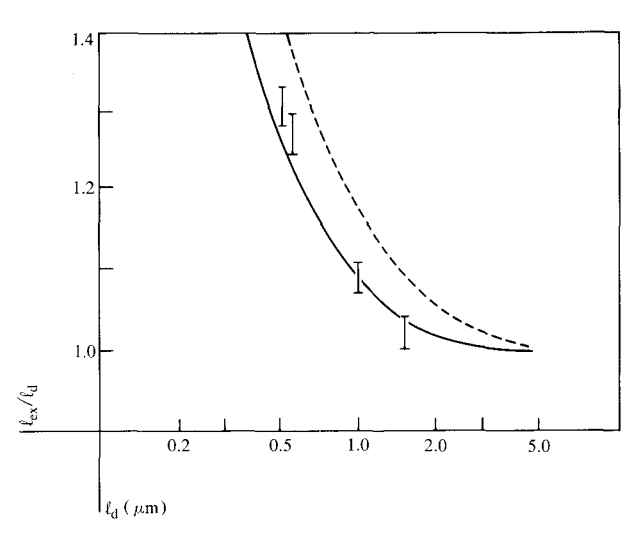


Figure 5 Calculated values [25] of the dimensional change $(\ell_{\rm ex}/\ell_{\rm d})$ necessary for proximity correction of isolated squares (----) and "infinite" lines (----) with widths $\ell_{\rm d}$. Experimental data, shown as error bars, are from [26].

are required to be equal, then solutions of these s equations for m < s unknowns can be obtained in a least-squares sense. As has been discussed above (see also Refs. [13a, 24]), such solutions are inherently ambiguous due to subjectiveness in the definition of sample points and due to the dependences of such solutions on initial "guesses" for a least-squares approximation. In spite of shortcomings, such a technique has its strength. Notably, it allows more sample points to be placed where the pattern is most critical, and fewer where it is less critical. Such a human interpretation of the pattern could be infeasible for a complex electron lithographic pattern. The use of sample points to optimize pattern data by dissecting shapes within a pattern into appropriate subshapes or segments has been discussed elsewhere [27].

A technique that is independent of the subjective interpretation of the pattern can be developed if $\tilde{\epsilon}$ [given by Eq. (3)] is used as a criterion for the magnitude of the proximity effect. If for each shape in the pattern one calculates $\tilde{\epsilon}_l$ and imposes it to be equal to, e.g., $\tilde{\epsilon}_0$ for all shapes in the pattern, one obtains a system of m linear equations:

$$\bar{\varepsilon}_0 = \sum_{I=1}^m n_I \int_{A_I} \int_{A_J} f(r_{ij}) dA_j dA_I / A_I,$$

$$I = 1, 2, \dots, m. \tag{7}$$

These fully determined systems of m linear equations for the m unknowns (n_i) can be solved exactly. Thus, the strength of this *self-consistent* technique [8] is that a unique solution is obtained which is independent of any

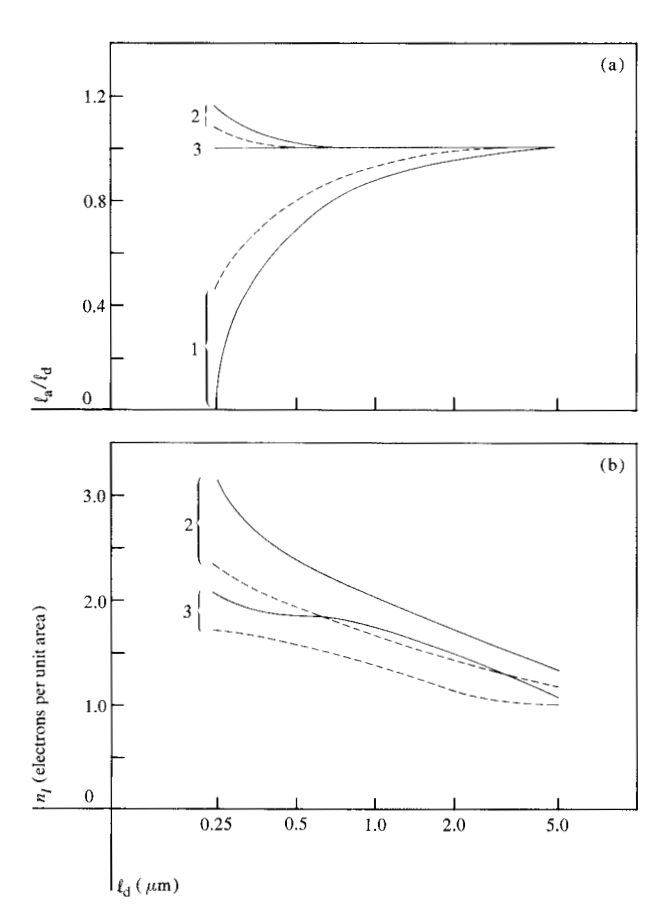


Figure 6 (a) Dimensional deviation (ℓ_a/ℓ_d) for isolated squares (—) and lines (---) of designed widths ℓ_d in the case of uncorrected patterns (Curves 1) and patterns corrected via the self-consistent technique (area averaged correction—Curves 2) and the algorithm given in the Appendix (edge adjustment correction—Curve 3). (b) Corresponding exposure values n_t . The proximity function parameters are $\beta_t = 0.1 \ \mu \text{m}$; $\beta_b = 2.5 \ \mu \text{m}$; $\eta_E = 0.9 \ \mu \text{m}$; $\eta_E =$

subjective and ambiguous interpretation of the pattern. It should be noted that the quality of corrections depends on the pattern data used in the solution of Eq. (7). While good corrections are found (vide infra) where shapes of approximately similar sizes comprise a pattern, it is found [28, 29] that subdivision of large shapes is necessary in certain cases for adequate proximity correction.

Nevertheless, the technique has a shortcoming. It considers the value of ε at each point in each shape in the pattern democratically. Since the value of ε at certain points (e.g., along the periphery or at a corner) of a shape may be more critical than at other points (e.g., within an interior of a large shape), an unequal weighting of parts of a pattern may have to be considered.

In principle, the value of ε at critical locations in a shape can be considered explicitly. Several algorithms [13a, 24, 30] have been proposed. Two of these rely on the calculation of ε at certain sample points [24] or within certain regions [13a] along the periphery of shapes in a pattern. Such calculations are in addition to the calculation of ε or $\bar{\varepsilon}_I$ in the interior of a shape. Thus this additional constraint, without any additional degrees of freedom (i.e., one incident electron exposure value per shape), leads to an overdetermined system of equations. Once again, the solutions can be obtained in the least-squares sense, with all the concomitant ambiguities.

Another algorithm that avoids such ambiguities by remaining within the self-consistent framework [30] considers the values of ε at a point A located midway along the side of length 2a of a rectangle of width 2b. It can be shown (Appendix 1) that 1) the value ε at point A, ε_A , decreases as the dimension of an isolated uncorrected shape decreases. This leads to the well-known underdevelopment of smaller isolated shapes as compared to the large shapes. 2) The self-consistent algorithm given by Eq. (7) leads to an "overcompensation." That is, while perfect compensation should yield ε_{A} independent of a, the values of n_i obtained from the solution of Eq. (7) lead to values of ε_{Λ} that depend on (increase with) a. 3) This overcompensation can be exactly corrected for isolated shapes by the multiplication of n, by a factor F given by Eq. (A6) in the Appendix. Results for isolated squares and lines, Fig. 6(a), shown in terms of the dimensional deviation ℓ_a/ℓ_d , indicate that "perfect" compensation is achieved. Corresponding values of incident exposure n_i are shown in Fig. 6(b). In the case of geometries involving intershape proximity effects, the overcorrection due to the self-consistent technique is again reduced [30] significantly by use of the factor F. Note that the self-consistent technique seems to significantly overcompensate only for dimensions $<0.5 \mu m$.

Comparisons

The strengths and weaknesses of correction algorithms can be summarized as follows. Algorithms that *adjust* pattern dimensions, though favored on the basis of compatibility with electron lithographic hardware, have shortcomings. First, the corrections are extremely difficult and probably impossible to calculate for arbitrary patterns. For simple patterns, calculations have been possible and table look-up schemes have sometimes been developed to avoid computational complexities. Note, however, that a table look-up scheme would be inadequate for a pattern of the type where rectangles of approximately the same size suffer from significant intershape proximity effects in some locations [e.g., rectangle F in Fig. 1(a)] but experience very little effect in others [e.g., rectangle C in Fig.

1(a)]. This can be better understood by considering the value of ε through a cross-section of an isolated line (Fig. 7). If the development level, as defined by a large shape, is set at $\varepsilon \approx 0.5$, the uncorrected linewidth $\ell_{\rm u}$ will be significantly narrower than the designed linewidth $\ell_{\rm d}$. Increasing the linewidth of the exposed line $\ell_{\rm ex}$ can also yield a developed shape with the correct dimension. However, such a shape is quite sensitive to the development level ε ; an increase in ε from ≈ 0.5 to 0.6 would lead to serious underdevelopment. This has been demonstrated by experiments involving the sensitivity of this technique to development conditions [26].

The algorithm that adjusts incident electron exposures can yield not only the correct value of ε at the designed edge, but also (through greater slope of ε in Fig. 7) less sensitivity to the developer. This relative insensitivity to small errors in the development conditions is a significant strength of any technique that adjusts incident exposures. An additional strength of such an algorithm is in its applicability to arbitrary patterns. In our experience the computing time for corrections for arbitrary patterns is found (see details in the next section) to be comparable to or less than the time for post-processing of such patterns generated by means of a computer-aided design system. Since the quality of corrections obtained via an exposureadjustment algorithm depends on the partitioning of the pattern into elementary shapes, some special decomposition of the pattern is found to be necessary [28, 29] for certain types of patterns. Finally, it should be noted that while there exists no means to explicitly control incident electron exposure in regions outside of those addressed by the e-beam, some special consideration for exposure near edges of shapes must be considered, e.g., through algorithms discussed in the Appendix.

Experimental results

The most important requirement of any proximity effect correction technique is that it yield "adequate" corrections for all shapes in the pattern. While not all of the above mentioned algorithms have as yet been experimentally evaluated, enough evidence exists to form some tentative conclusions.

Experimental results for algorithms involving adjustment to pattern dimensions have been reported [24, 26] using table "look-up" and "contour-fitting" schemes. In the former case, simple patterns (lines and pads) were exposed with appropriate dimensions that were determined a priori from experiment and stored in several tables. The exposed patterns with the corrected dimensions are reported to be within $\pm 0.1~\mu m$ of the design. In the latter technique, ε values at sample points along the "contour" of a shape were calculated. Using a least-squares tech-

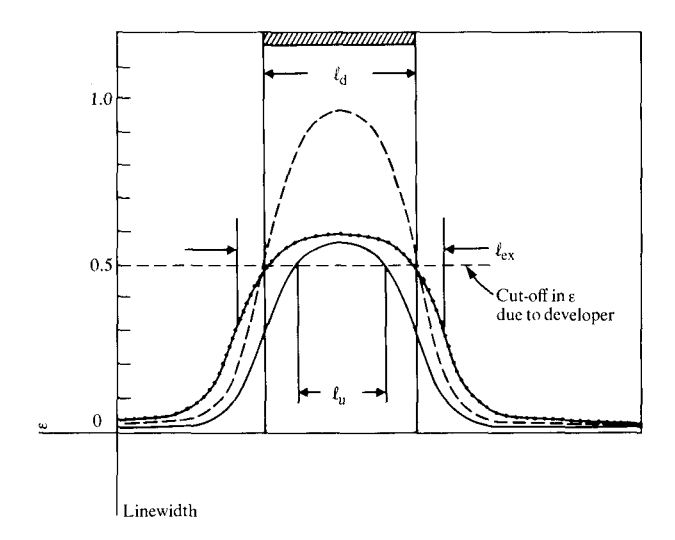
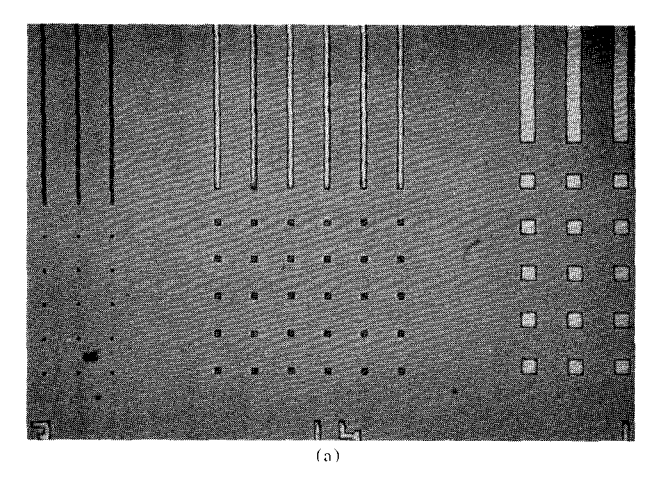


Figure 7 Schematic of ε through an isolated line of width ℓ_d for an uncorrected pattern (——); for a proximity-corrected pattern via a dimension adjustment technique (—•—•—); for a proximity-corrected pattern via an exposure adjustment technique (———).

nique, pattern dimensions (as well as exposures) were varied until ε values along the contour were approximately uniform. An algorithm has recently been reported [31] which is applicable to a large pattern and which considers adjustments to both pattern dimension and exposure; pattern fidelity of 0.2 μ m seems to be evident.

Experimental results for patterns involving adjustment of incident electron exposure are more extensive. The first reported [8] proximity correction technique used was the self-consistent algorithm [Eq. (7)]; numerous experimental results using this technique have been reported. Another similar exposure adjustment technique has also been reported [32]. Results for simple patterns have shown improvement in pattern fidelity. Rounding at corners of shapes was avoided by computing different exposures in elemental areas along corners and the periphery of shapes. Exposure adjustments have also been determined [33] via a Monte Carlo calculation of exposures within a resist pattern defining a source/drain region of an FET.

The self-consistent technique has been used [8, 13c, 34, 35] on a variety of patterns and under a variety of experimental conditions. Intrashape proximity effects lead to incomplete development of smaller shapes [see for example the 1- and 2- μ m squares and lines in Fig. 8(a)], while all larger shapes have developed completely. Here, as in all results presented below, the development conditions [13c] are chosen such that the largest shapes in the pattern (typically a 5- μ m line) are fully- but *not* over-devel-



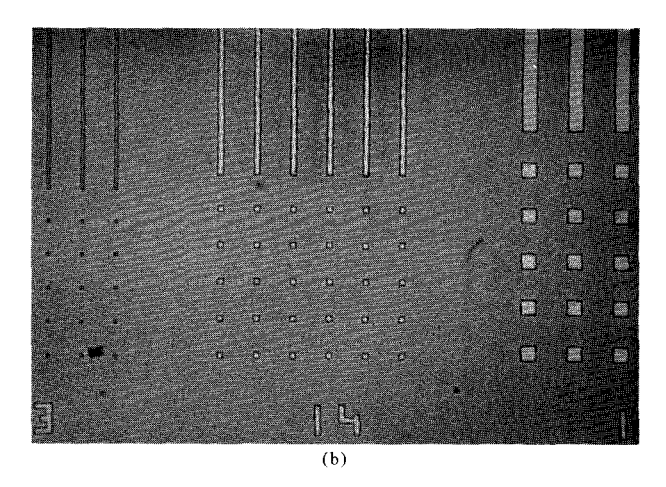


Figure 8 Optical micrographs showing (a) the uncorrected and (b) SPECTRE-corrected pattern consisting of 1-, 2-, and 5- μ m squares and lines, all separated by 10 μ m.

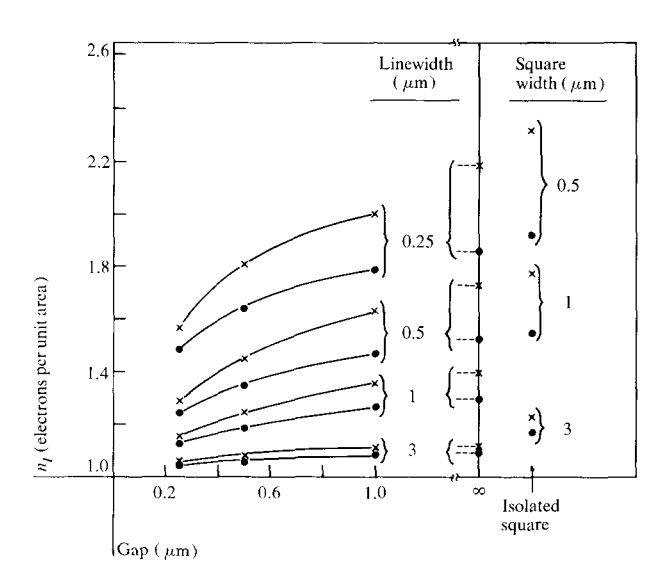


Figure 9 Incident electron exposure values necessary to correct for proximity effects in a pattern consisting of a collection of lines with a variety of widths and spacings between lines. Note that incident electron exposures are normalized to unity for an infinitely large area. The proximity function parameters are $\beta_t = 0.1 \ \mu m$; $\beta_b = 1.0 \ \mu m$; $\eta_E = 0.6 \ (\bullet)$ or $1.0 \ (\times)$.

oped. This development criterion makes realistic comparison between corrected and uncorrected patterns. The corrected pattern is shown in Fig. 8(b); notice that complete development of all parts of the pattern without measurable (<0.1- μ m) error in pattern dimensions is obtained. The proximity function parameters used in this case were $\beta_f = 0.1 \ \mu$ m, $\beta_b = 1.0 \ \mu$ m, and $\eta_E = 0.6$. Exposure values that were obtained from the solution of Eq.

(7) are shown in Fig. 9 for two sets of proximity function parameters and for patterns consisting of a collection of lines with 0.25-, 0.5-, 1-, and $3-\mu m$ widths and gaps between lines. Exposures for isolated lines and squares are also shown. Note that exposures using the correction discussed in Appendix 1 have not been shown. They can be easily obtained by multiplication of the values from Fig. 9 with the factor F from the Appendix. [At present, no experimental evaluation of this new correction algorithm has been performed.]

A program package called SPECTRE (for Self-consistent Proximity Effect Correction Technique for Resist Exposure) has been developed [8, 13c] that takes as its input pattern data and the parameters for the proximity function. Without any interpretation of the pattern data, the program outputs pattern data with appended values for exposure changes. Since the e-beam machine hardware stipulates only one exposure value (or scan speed) per shape, SPECTRE computes only one exposure value per shape. A flowchart for the SPECTRE program package [13c] is shown in Fig. 10. An interactive program (SPECREAD) accepts user inputs regarding e-beam machine and pattern parameters. The pattern is divided into various zones (via ZONMAP) based on whether proximity corrections are to be performed on all shapes (if the pattern is nonrepeating) or whether only some shapes are to be corrected (if the pattern is repeating) and the results replicated to the rest of the repeating pattern. The program TAGSHP tags each shape in the pattern according to the zone it belongs in. The tagged pattern data are sorted (via SORT) and then passed to the main computing program (COMPC) for automatic exposure calculations of each shape via the solution of Eq. (7) for one zone at a time. The typical computation time we obtained [8, 13c] for every shape in an arbitrary pattern consisting of 10^4 rectangular shapes using an IBM 370/168 computer (4Mbyte configuration) was $\approx 10^2$ s, increasing linearly with the number of shapes. The memory requirement for execution of the program is less than 256K bytes.

The quality of corrections obtained using the self-consistent technique can be seen through the reexamination of Figs. 1(b-d). The uncorrected pattern shown in Fig. 1(a) was written by the e-beam machine as a set of 13 rectangular shapes shown in Fig. 1(c). Data for these shapes, after corrections using SPECTRE, yielded the improvement shown in Fig. 1(b). An alternate pattern data definition, shown in Fig. 1(d), in terms of 21 rectangular shapes, yielded almost identical patterns after corrections. Generally, pattern redefinition is unnecessary [34, 35] for proximity corrections using SPECTRE except in situations where large shapes are separated by a small gap [28] or where small shapes are in proximity with only some parts of a large or long shape [29].

SPECTRE has been used routinely for experimental studies on 1-µm MOSFET VLSI devices [34] (see Fig. 11). In the case of the 8K FET RAM, the final metal level was lithographically the most difficult. This was due to the requirement for a 1.3-\mum-thick PMMA resist in order to ensure lift-off of a $0.5-\mu m$ Al layer over a 500-nm topography; see Figs. 11 and 12. The parameters used here were $\beta_r = 0.1 \mu \text{m}$, $\beta_h = 1.0 \mu \text{m}$, and $\eta_F = 0.6$. The normalized exposure values used to correct this level, which consisted of $\approx 2.2 \times 10^4$ shapes, are shown in Fig. 12. Note that the exposure value increases considerably when a chip is reduced to half scale (yielding a 0.5- μ m feature). Typical results [35] for the case of $0.5-\mu m$ bubble lithography are shown in Fig. 13. The micrographs show gold patterns of "C bars" on polyimide substrates; these were obtained through the use of SPECTRE-corrected electron lithography. Thus, proximity correction is now routinely possible for practical submicron lithography.

Conclusion

The deleterious effect of electron scattering in the resist and substrate on the lithographic image fidelity has been reviewed. Phenomenologically, a proximity function has been developed and serves as a macroscopic measure of the extent of influence in the resist due to electron scattering. Modeling of such a function by a pair of Gaussian functions yields parameters that are amenable to physical interpretation and obtainable from experiment and theory.

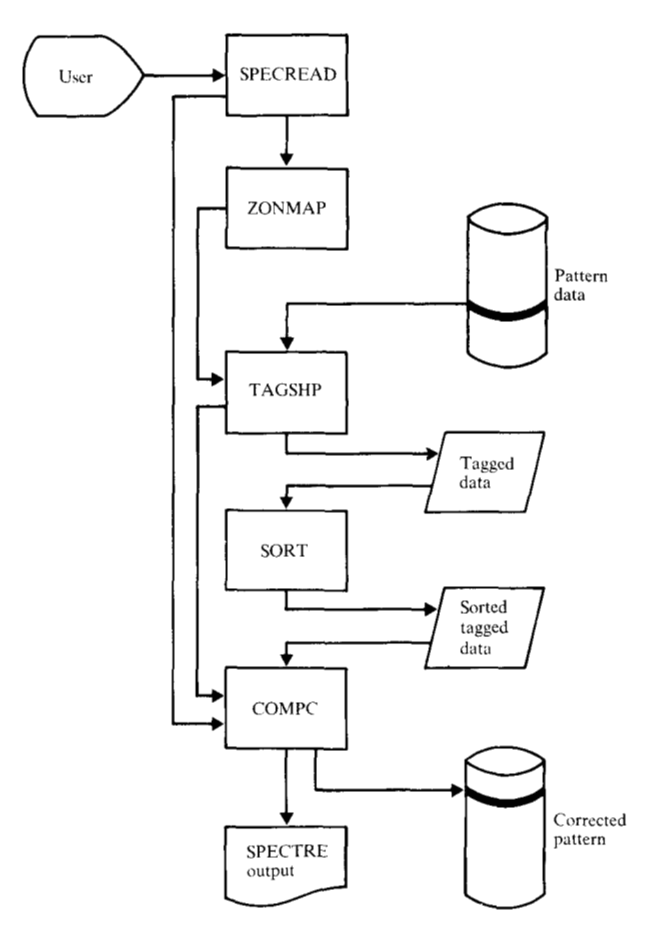
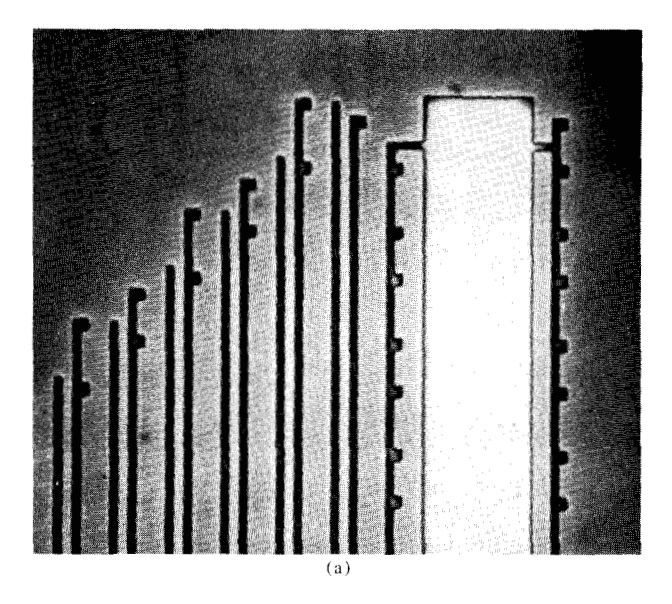


Figure 10 SPECTRE flowchart. See text and Ref. [13c] for details.

The magnitude of the proximity effect has been estimated through the use of the proximity function. This has also led to an understanding of the sensitivity or insensitivity of the parameters in the proximity function. Methods for decreasing proximity effects have also been predicted; existing sparse experimental data are consistent with these results. A variety of methods for correction of proximity effects have been outlined and the strengths and weaknesses of each have been reviewed. While techniques utilizing adjustment of pattern dimensions are attractive in terms of compatibility with electron lithographic machines that do not allow exposure adjustment, they seem to be practically implementable only with table "look-up" algorithms. Techniques involving adjustments of electron exposures require an e-beam machine capable of suitable exposure adjustments. These techniques have the strength of being readily implementable in the case of arbitrarily complex patterns, but the complexity of the pattern determines the computational requirements.



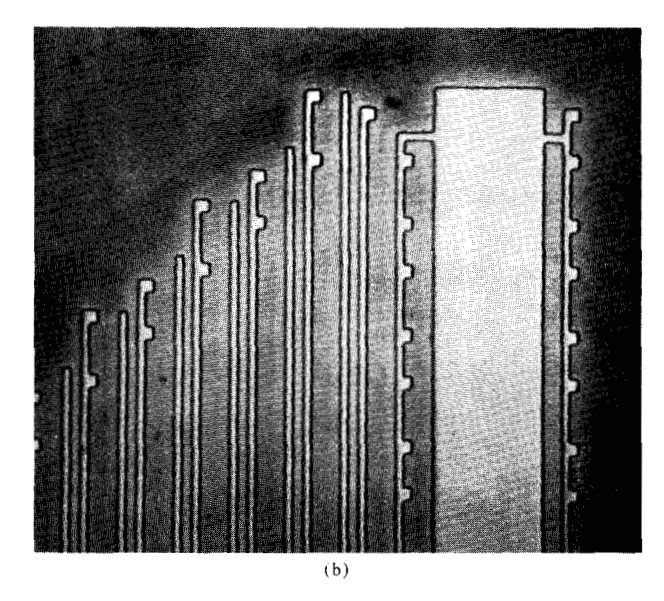


Figure 11 Optical micrographs of (a) uncorrected and (b) SPECTRE-corrected pattern from a 1-μm MOSFET lithography. (Courtesy of W. Grobman et al. [34].)

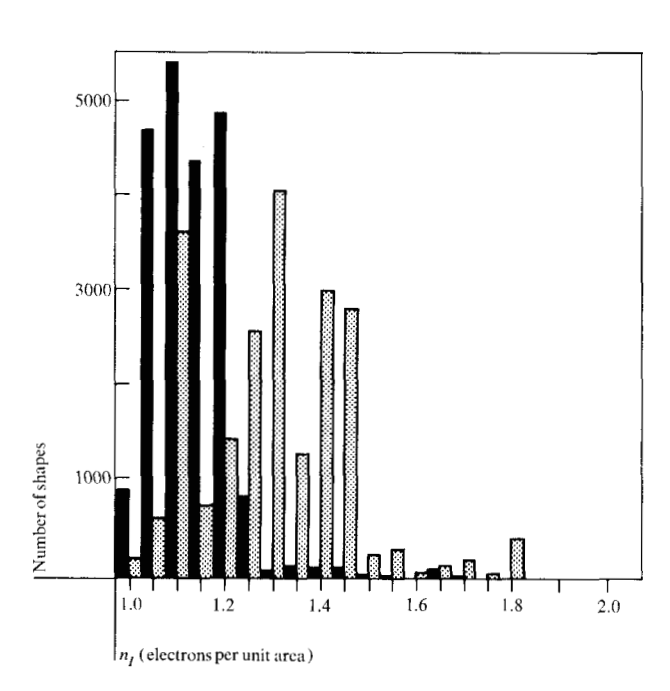


Figure 12 Distribution of exposure values for 1- μ m (black bars) and 0.5- μ m (shaded bars) lithography for SPECTRE-corrected pattern for the MOSFET lithography shown in Fig. 11. β_t = 0.1 μ m; β_b = 1.0 μ m; η_E = 0.6. (Courtesy of W. Grobman *et al.* [34].)

Experimental results have been reported using some of the algorithms described here. The table "look-up" and pattern-dimension adjustment seem to have been attempted only for simple patterns. Techniques using exposure adjustment, especially the self-consistent technique, have been more extensively tested. In particular, the program SPECTRE, through its ease of operation, has been successfully used for $1-\mu m$ FET and $0.5-\mu m$ bubble technologies.

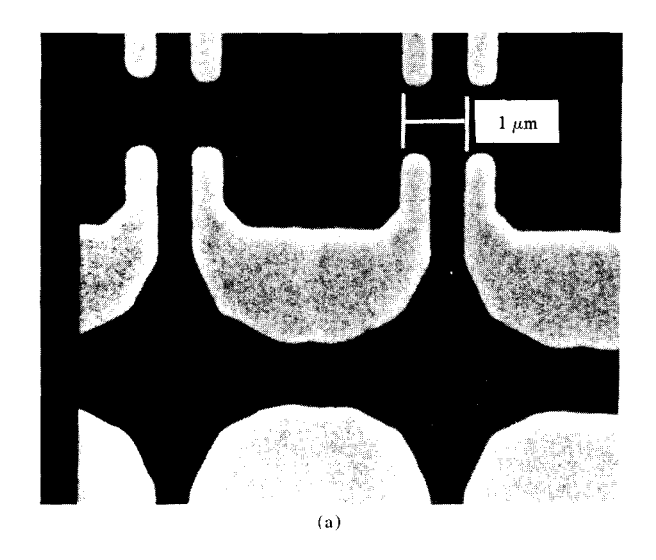
At present, several questions remain. For example, for any particular level of lithography, one wonders what ultimate resolution is attainable through the use of proximity correction techniques, or what minimum level of proximity corrections are imperative for any particular level of lithography. The sensitivity of the proximity function parameters to resist materials and thickness, developer, substrate, and e-beam machine conditions are as yet unknown. Clearly, further work is necessary.

Acknowledgments

I am thankful to many of my colleagues at IBM for stimulating discussions and support—in particular, A. N. Broers, T. H. P. Chang, T. Donohue, M. Hatzakis, D. Hofer, W. Grobman, D. F. Kyser, H. Luhn, E. Munro, A. Speth, C. Ting, and A. D. Wilson.

Appendix: An algorithm to reduce overcompensation of proximity effects in the self-consistent technique

The values of ε at points A and O in an isolated rectangle can be calculated via Eq. (2) for a particular form of the proximity function. Assuming for simplicity a single Gaussian (with characteristic width β), one obtains



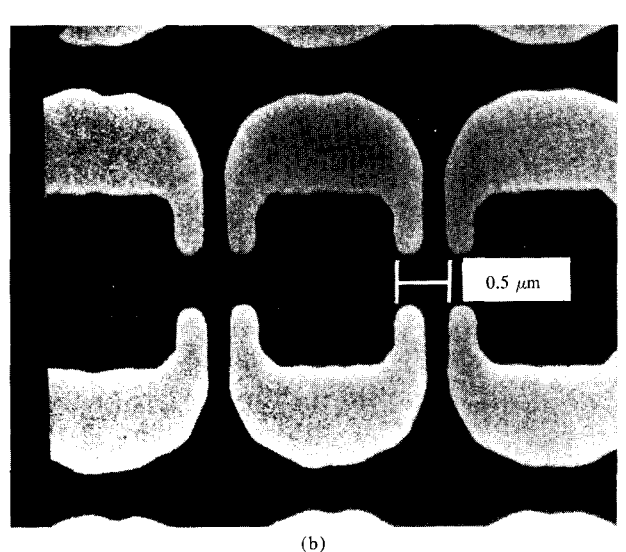


Figure 13 Scanning electron micrographs of (a) 1- μ m and (b) 0.5- μ m bubble-lithography-generated gold-plated x-ray masks on polyimide substrates. In the former case, note that 0.5- μ m gaps are accurately obtained; in the latter case the 0.25- μ m gaps are smaller than those designed. (Courtesy of D. Hofer *et al.* [35].)

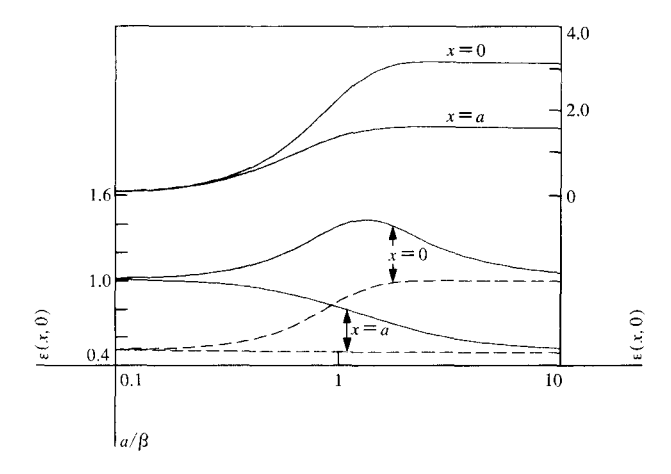


Figure A1 Upper part: Values of ε at points A and O in an isolated shape, given by Eq. (A1). Note the decrease in ε as a function of a due to an intrashape proximity effect. Lower part: Corrected values of ε at points A and O, obtained through the use of the self-consistent technique (——) and the "edge-compensation" technique (——).

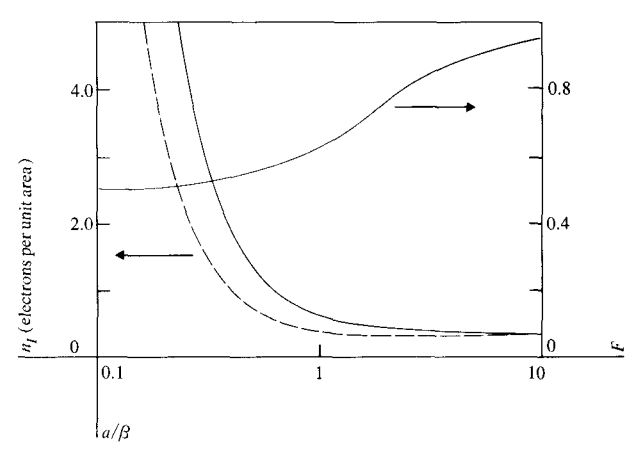


Figure A2 Values of exposure n_i in the self-consistent technique (—) and in the "edge-compensation" technique (——); the factor F, Eq. (A6), is also shown.

$$\varepsilon(A) = \pi/2\beta^2 \operatorname{erf} (b/\beta) \operatorname{erf} (2a/\beta),$$

 $\varepsilon(O) = \pi\beta^2 \operatorname{erf} (b/\beta) \operatorname{erf} (a/\beta).$ (A1)

For isolated squares (with b = a), computed values (Fig. A1) show the expected decrease in $\varepsilon(A)$ with decreasing a. This leads to the underdevelopment of small isolated shapes as compared to larger shapes.

Using the "self-consistent" technique, a value of incident electron exposure n_I can be calculated. Solution of

Eq. (7), with the constraint that $\bar{\varepsilon}_I = \varepsilon_0$, a constant, for all shapes (i.e., independent of a) yields

$$n_I = \frac{4ab\varepsilon_0}{\pi\beta^4 H(\beta)} ,$$

where

$$H(\beta) = [1/\sqrt{\pi} - Q(2a/\beta)][1/\sqrt{\pi} - Q(2b/\beta)]$$
 (A2)

and

$$Q(x) = x \operatorname{erf}(x) + 1/\sqrt{\pi} \exp(-x^2).$$

The value of ε at a point A, $\varepsilon^{\varepsilon}(A)$, in the shape exposed with the exposure n_i is thus

$$\varepsilon^{c}(\mathbf{A}) = n_{i}\varepsilon(\mathbf{A}). \tag{A3}$$

Computed values for $\varepsilon^{c}(A)$ show (Fig. A1) that ε increases with decreasing a. Clearly, one would prefer $\varepsilon(A)$ to be independent of a; thus, the "self-consistent" technique leads to an overcompensation.

This overcompensation can be ameliorated by multiplying n, by a factor F given by

$$F = \frac{\varepsilon_0}{n_t \varepsilon(A)}.$$
(A4)

The behavior of F and n_i as functions of a is shown in Fig. A2. For isolated shapes, this factor leads to a perfect compensation, since the corrected value of ε , $\varepsilon^{EC}(A)$, is given by

$$\varepsilon^{\text{EC}} = n_i F_{\varepsilon}(\mathbf{A}),\tag{A5}$$

which is completely independent of a.

For a realistic proximity function, defined by the two-Gaussian-function equation (1), the factor F can be easily generalized:

$$F = \frac{1}{4ab} \frac{\left[\beta_{\rm f}^2 H(\beta_{\rm f}) + \eta_{\rm E} \beta_{\rm b}^2 H(\beta_{\rm b})\right]}{\left[G(\beta_{\rm f}) + \eta_{\rm E} G(\beta_{\rm b})\right]}.$$
 (A6)

$$G(\beta_i) = \operatorname{erf}(b/\beta_i) \operatorname{erf}(2a/\beta_i).$$

Figure 6 showed some results obtained using this "edgecompensation" factor. For isolated squares and lines, the compensation is perfect [at least in terms of ensuring that $\varepsilon(A)$ is independent of a], while for shapes adjacent to other shapes, a significant reduction in overcompensation is achieved.

References and note

- 1. M. Hatzakis, "New Method of Observing Electron Penetration Profiles in Solids," Appl. Phys. Lett. 18, 7 (1971).
- 2. E. D. Wolf, F. S. Ozdemir, W. E. Perkins, and P. J. Coane, "Response of the Positive Electron Resist, Elvacite 2041, to Kilovolt Electron-Beam Exposure," Record of the Eleventh Symposium on Electron, Ion, and Laser Beam Technology, Boulder, CO, 1971; R. F. M. Thornley, Ed., San Francisco Press, CA; IEEE Catalog No. 71, C23-ED, pp. 331-336.
- 3. R. F. Herzog, J. S. Greeneich, T. E. Everhart, and T. Van Duzer, "Computer-Controlled Resist Exposure in the Scanning Electron Microscope," IEEE Trans. Electron Devices ED-19, 635 (1972).
- 4. James S. Greeneich and Theodore Van Duzer, "An Exposure Model for Electron-Sensitive Resists," IEEE Trans. Electron Devices ED-21, 286 (1974).
- 5. R. J. Hawryluk, Henry I. Smith, A. Soares, and Andrew M. Hawryluk, "Energy Dissipation in a Thin Polymer Film by Electron Beam Scattering Experiment," J. Appl. Phys. 46, 2528 (1975).

- 6. D. F. Kyser and K. Murata, "Monte Carlo Simulation of Electron Beam Scattering and Energy Loss in Thin Films,' Proceedings of the Sixth International Conference on Electron and Ion Beam Science and Technology, San Francisco, CA, 1974; R. Bakish, Ed., The Electrochemical Society, Princeton, NJ, pp. 205-223.
 T. H. P. Chang, "Proximity Effect in Electron Beam Lith-
- ography," J. Vac. Sci. Technol. 12, 1271 (1975).
- M. Parikh, "SPECTRE-A Self-Consistent Proximity Effect Correction Technique for Resist Exposure," J. Vac. Sci. Technol. 15, 931 (1978).
- 9. Shapes are defined to be those entities that make up a pattern. For example, if the letter V were to be written by the ebeam machine as a composite of two parallelograms and one triangle, these three entities would be considered shapes.
- 10. D. F. Kyser and N. S. Viswanathan, "Monte Carlo Simulation of Spatially Distributed Beams in Electron Beam Lithography," J. Vac. Sci. Technol. 12, 1305 (1975).
- 11. R. E. Jewett, T. I. Hagouel, A. R. Neureuther, and T. Van Duzer, "Line-Profile Resist Development Simulation Techniques," *Polymer Eng. Sci.* 17, 381 (1977).
- 12. W. D. Grobman and A. J. Speth, "An Exposure Wedge for Electron Beam Lithography Development Control and for the Determination of Resist Development and Proximity Parameters," Proceedings of the Eighth International Conference on Electron and Ion Beam Science and Technology, Seattle, WA, 1978; R. Bakish, Ed., The Electrochemical Society, Princeton, NJ, Proceedings Vol. 78-5, p. 276.
- 13. M. Parikh, "Corrections to Proximity Effects in Electron Beam Lithography. (a) I. Theory, (b) II. Implementation, and (c) III. Experiment, J. Appl. Phys. 50, 4371, 4378, and 4383 (1979).
- 14. M. Parikh and D. F. Kyser, "Energy Deposition Functions in Electron Resist Films on Substrates," J. Appl. Phys. 50, 1104 (1979).
- A. R. Neureuther, D. F. Kyser, and C. H. Ting, "Electron Beam Resist Edge Profile Simulation," IEEE Trans. Electron Devices ED-26, 686 (1979).
- 16. William T. Scott, "The Theory of Small-Angle Multiple Scattering of Fast Charged Particles," Rev. Mod. Phys. 35, 231 (1963).
- 17. (a) James S. Greeneich, Burroughs Corporation Technical Center, 16701 W. Bernardo Dr., San Diego, CA, private communication, August 1978; (b) J. S. Greeneich, "The Impact of Electron Scattering on Linewidth Control in Electron Beam Lithography," Record of the Fifteenth Symposium on Electron, Ion, and Laser Beam Technology, Boston, MA, 1979; T. H. P. Chang, Ed., American Vacuum Society, American Institute of Physics, New York, to be published.
- 18. Fletcher Jones and Michael Hatzakis, "Experimental Determination of the Effect of Back-Scattered Electrons on the Dissolution Rate of PMMA," Ref. 12, loc. cit., p. 256.
- 19. M. S. Chung and K. L. Tai, "Investigations of Electron-Beam Resist Interactions in Electron Lithography," Ref. 12, loc. cit., p. 242.
- 20. Naoshi Sugiyama, Naoaki Aizaki, Akira Kawagi, and Yasuo Tarui, "A Data Processing System for Electron Lithography," Ref. 12, loc. cit., p. 184.
- 21. M. Parikh, "Dependence of Pattern Dimensions on Proximity Functions in Electron-Beam Lithography," J. Appl. Phys. 51, 700 (1980).
- 22. D. F. Kyser and C. H. Ting, "Voltage Dependence of Proximity Effects in Electron Beam Lithography," Ref. 17b, loc.
- 23. D. F. Kyser and M. Parikh, "Decrease in Proximity Effect by Sandwiching Thin Heavy Metal Films between Resists and Substrates," IBM Tech. Disclosure Bull. 21, 2496
- 24. N. D. Wittels and C. I. Youngman, "Proximity Effect Correction in Electron-Beam Lithography," Ref. 12, loc. cit., p. 361.

- 25. M. Parikh, "Calculation of Changes in Pattern Dimensions to Compensate for Proximity Effects in Electron Lithography," J. Appl. Phys. 51, 705 (1980).
- H. Sewell, "Control of Pattern Dimensions in Electron Lithography," J. Vac. Sci. Technol. 15, 927 (1978).
- M. Parikh, "Technique for Automatic Subdivision of Pattern Data for Enhanced Proximity Effect Corrections," *IBM Tech. Disclosure Bull.* 21, 4278 (1979).
- 28. W. D. Grobman, A. J. Speth, and T. H. P. Chang, "Proximity Correction Enhancements for 1-μm Dense Circuits," *IBM J. Res. Develop.* 24 (1980, this issue).
- M. Parikh and D. E. Schreiber, "Pattern Partitioning for Enhanced Proximity-Effect Corrections in Electron-Beam Lithography," IBM J. Res. Develop. 24 (September 1980), in press.
- M. Parikh, "Method for Computing Incident Electron Exposure Values to Compensate for Proximity Effects," IBM Tech. Disclosure Bull. 22, 2863 (1979).
- 31. A. Kikuchi, A. Kanamaru, and O. Nobumichi, "A Fast Computation Method for Exposure Intensity and Pattern Correction in Electron Beam Lithography," Ref. 17b, loc. cit.
- H. I. Ralph and H. Sewell, "Computer Control of Proximity and Size Effects in Electron Lithography," Ref. 12, loc. cit., p. 354.

- Hidefumi Nakata, Takaaki Kato, Kenji Murata, and Koichi Nagami, "Proximity Effect in FET Fabrication with Electron Beam Lithography," Ref. 12, loc. cit., p. 393.
- tron Beam Lithography," Ref. 12, loc. cit., p. 393.

 34. W. D. Grobman, H. E. Luhn, T. P. Donohue, A. J. Speth, A. Wilson, M. Hatzakis, and T. H. P. Chang, "1 \mu m MOSFET VLS1 Technology: Part VI—Electron Beam Lithography," IEEE Trans. Electron Devices ED-26, 360 (1979) and IEEE J. Solid State Circuits SC-14, 282 (1979).
- 35. D. C. Hofer, J. V. Powers, and W. D. Grobman, "X-Ray Lithographic Patterning of Magnetic Bubbles with Submicron Dimensions," Ref. 17b, loc. cit.

Received October 4, 1979; revised March 3, 1980

The author is located at the IBM Research Division laboratory, 5600 Cottle Road, San Jose, California 95193.